

Convex Programming Based Robust Localization in NLOS Prone Cluttered Environments

Sarfraz Nawaz
Oxford University Computing Laboratory
Parks Road, Oxford OX1 3QD
Sarfraz.Nawaz@comlab.ox.ac.uk

Niki Trigoni
Oxford University Computing Laboratory
Parks Road, Oxford OX1 3QD
Niki.Trigoni@comlab.ox.ac.uk

ABSTRACT

In a large variety of industrial scale processes, fixed or mobile sensors are typically deployed in large-scale vessels to monitor parameters such as temperature, pressure and chemical concentration. When these vessels are cluttered with obstacles, e.g. large cooling ponds cluttered with nuclear waste containers, it becomes increasingly difficult for the sensors to estimate their position. The acoustic ranging signals used for estimating distances between each sensor node and reference nodes fixed to the vessel infrastructure can suffer from Non-Line-Of-Sight (NLOS) signal propagation and thus introduce large positive errors in some of the estimated distances.

In this paper we present a robust localization algorithm for localizing sensors in cluttered NLOS environments. We show that if the number of erroneous range measurements is less than half, it is possible to accurately estimate these NLOS errors at each sensor node by solving a convex optimization problem. Each sensor node can then use its estimate of NLOS errors to accurately localize itself. Our approach is completely independent of the physical hardware used to perform range measurements and thus can be used to localize sensor nodes in any NLOS prone environment. We demonstrate this with the help of experimental results with three different hardware platforms each employing a different ranging mechanism.

Categories and Subject Descriptors

C.2.0 [Computer-Communication Networks]: General;
I.0 [Computing Methodologies]: General

General Terms

Algorithms, Experimentation, Reliability

Keywords

Localization, Non-line-of-sight, Ranging

Permission to make digital or hard copies of all or part of this work for personal or classroom use is granted without fee provided that copies are not made or distributed for profit or commercial advantage and that copies bear this notice and the full citation on the first page. To copy otherwise, to republish, to post on servers or to redistribute to lists, requires prior specific permission and/or a fee.

IPSN'11, April 12–14, 2011, Chicago, Illinois.

Copyright 2011 ACM 978-1-4503-0512-9/11/04 ...\$10.00.



(a) Storage pond



(b) Robot Prototype

Figure 1: Sensor nodes for industrial processes. Robot prototype photograph provided by Simon Watson from the University of Manchester.

1. INTRODUCTION

There is a large variety of industrial scale aqueous processes that are carried out in very large scale vessels or tanks. For example, in chemical industry, different chemical reactions are carried out in large enclosed reaction vessels and chemical engineers are generally interested in temperature, pressure, turbidity and other parameters inside the vessel. Currently available methods which place sensors outside the vessel are not only limited in which parameters can be measured but also in the spatial and temporal resolution. There are some processes where industrial waste is stored underwater in large ponds of water. For example, in nuclear industry, when spent nuclear fuel is taken out of the nuclear reactor, it continues to generate heat for a very long period of time. This waste is stored in metallic containers which are then kept inside a large cooling pond for 60 to 100 years before the waste can be disposed off permanently. These cooling ponds can be as large as 50m×20m and as deep as 15m. One such storage pool is shown in Fig. (1a) where a Manhattan landscape of skip towers can be easily seen. During this extended period, these ponds must be carefully monitored for temperature hot-spots, radioactivity and leaks.

For monitoring these aqueous industrial processes, we have proposed an underwater mobile sensor network. Fig. (1b) shows a prototype of our mobile sensor node. Each sensor node is just 10cm in diameter and has five degrees of freedom for easy maneuvering through the clutter environment. It will be equipped with temperature, pH, turbidity and radioactivity sensors and ultrasound transducers for acoustic communication and ranging to both other sensor nodes and reference nodes fixed to the vessel infrastructure. A swarm of these sensor nodes can be introduced in a reaction vessel

or a cooling pond to monitor the conditions inside these environments. For the robots to sense and explore the pools, they must be able to determine their positions in these underwater environments. However, the cluttered nature of these environments presents us with unique challenges. The ultrasound pulses used for performing range measurements can reflect and bounce off the metallic surfaces before arriving at the transducers. These multipath reflections introduce large positive errors in some of the estimated distances between the reference and sensor nodes as shown in Fig. (2). These erroneous measurements make it very difficult to estimate the true positions of sensor nodes. The main focus of this work is to develop a robust localization approach that would allow these sensor nodes to localize themselves accurately in such cluttered environments even in the presence of erroneous measurements.

The current body of research generally addresses this problem by identifying the Line-of-Sight (LOS) and Non-Line-of-Sight (NLOS) range measurements [25, 17]. The erroneous measurements are then either removed completely or assigned smaller weights while calculating the coordinates of the sensor node. The identification of LOS and NLOS measurements generally relies on the characteristics of the received signals at the physical layer [24]. Therefore, it is specific to the modality used to perform ranging and cannot be used across different hardware platforms. Another approach is to characterize the target environment by performing extensive pre-deployment measurements [18, 23]. This prior information is then used to weight the measurements during localization. However, this approach is environment dependent and cannot be used for ad-hoc deployments. There is also some research that treats the NLOS range measurements as outliers [9]. This approach tries to detect and remove these outliers by observing the consistency of the measurements. However, even if this outlier detection is completely successful, removing measurements lowers the overall localization accuracy.

In this paper, we present a robust localization algorithm that overcomes all of the above mentioned issues. Although, we have used aqueous industrial processes as our motivation, our approach can be used to localize sensor nodes in any of the NLOS prone environments. Following are the primary contributions of our work,

- We propose a robust localization algorithm that is completely independent of the physical signals used to perform range measurements and does not require any prior knowledge about the environment.
- We analyze the robustness of our algorithm and quantify its breaking point, that is, the largest percentage of non line of sight range measurements that it can tolerate. We show that by exploiting the assumption that non line of sight errors are typically positive we can shift the breaking point from 30% to 50% in the asymptotic case.
- We compare our robust localization algorithm with seven competing algorithms, including an oracle algorithm that can perfectly distinguish between line of sight and non line of sight measurements. We present experimental results from a series of real sensor network testbeds: 1) a lecture theater using Jennic nodes and ToF radio ranging; 2) a meeting room with MIT Cricket

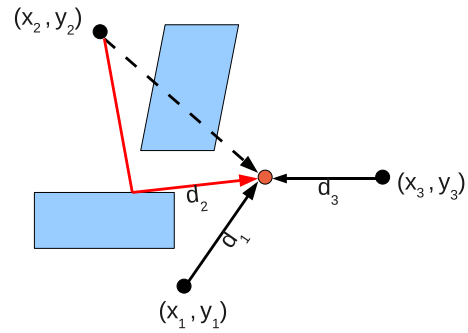


Figure 2: Non line of sight signal propagation in a cluttered environment results in an overestimated distance measurement d_2

nodes and acoustic ranging; and 3) a water tank using Neptune [2] and SenseComp [3] transducers and acoustic ranging.

- Besides real experiments with fixed sensor nodes, we have conducted simulations with mobile sensor nodes. In mobile scenarios, filters are typically used to fuse noisy position measurements over time, and produce trajectories that tend to be close to the real ones. We show that our robust localization algorithm used without any filter significantly outperforms competing algorithms (e.g. non linear least squares), even when the position estimates are fused with an Extended Kalman Filter.

The rest of this paper is organized as follows. Section 2 outlines the localization problem that this work is addressing. Section 3 shows that traditional localization algorithms cannot localize sensor nodes accurately in the presence of NLOS measurements. Section 4 presents our robust localization algorithm. Section 5 presents an analysis of the robustness of our algorithm. Section 6 and 7 describe experimental results for fixed and mobile sensor nodes respectively. Related work is discussed in Section 8 and, finally, Section 9 concludes this paper.

2. PROBLEM SET UP

For ease of exposition, we will restrict ourselves to two dimensions, however, the ideas and the solutions presented in this paper can be easily extended to the complete three dimensional case. Let us suppose that there are m fixed reference nodes with coordinates (x_i, y_i) where $i = 1, 2, \dots, m$. A sensor node that wishes to determine its coordinates, estimates its distance to three or more reference nodes as shown in Fig. (2). Let us suppose that d_i is the estimated distance to reference node i . Each estimated distance d_i is given as,

$$\bar{d}_i = d_i - \bar{n}_i - \bar{e}_i \quad i = 1, 2, \dots, m \quad (1)$$

where \bar{d}_i is the true distance, \bar{e}_i is a small measurement error and \bar{n}_i is a large positive error introduced due to non line of sight signal propagation. If there is a direct path available between the reference and the unlocalized node then $\bar{n}_i = 0$ for this range measurement. We assume that the measurement error \bar{e}_i has a zero mean Gaussian distribution, where as the non line of sight error \bar{n}_i is drawn from any non-negative distribution.

$$\bar{\epsilon}_i \sim \mathcal{N}(0, \sigma^2) \quad (2)$$

where σ is the standard deviation of the Gaussian distribution. In literature, NLOS errors are assumed to follow a uniform or an exponential distribution. However, our approach is independent of the NLOS error distribution. The only assumption that we make is that these errors follow a non-negative distribution.

Given the reference node coordinates (x_i, y_i) and the measured distances d_i with $i = 1, 2, \dots, m$ between the reference nodes and the unlocalized node, determine the coordinates of the unlocalized node (x, y) where some of the distances are overestimated due to non line of sight signal propagation and there is no additional information available to distinguish these erroneous measurements from the rest of the direct line of sight range measurements.

3. ISSUES WITH THE TRADITIONAL APPROACH

In this section, we outline the traditional least squares based localization approach and analyze its performance in the presence of overestimated distances due to non line of sight signal propagation. If (x, y) are coordinates of the unlocalized node, then we can write a system of equations as,

$$\begin{aligned} (x_1 - x)^2 + (y_1 - y)^2 &= d_1^2 \\ (x_2 - x)^2 + (y_2 - y)^2 &= d_2^2 \\ &\vdots \\ (x_m - x)^2 + (y_m - y)^2 &= d_m^2 \end{aligned} \quad (3)$$

The only unknowns in the above system of equations are the coordinates x and y of the unlocalized node. These can be determined by solving a problem that is known as *least squares* and is given as

$$\hat{\mathbf{x}} = \underset{\mathbf{x}}{\operatorname{argmin}} \sum_{i=1}^m r_i(\mathbf{x})^2 \quad (4)$$

where $\mathbf{x} = [x, y]^T$, $\hat{\mathbf{x}}$ is a vector of estimated coordinates and $r_i(\mathbf{x})$ is a residual function given as,

$$r_i(\mathbf{x}) = \{(x_i - x)^2 + (y_i - y)^2\} - d_i^2 \quad i = 1, 2, \dots, m \quad (5)$$

This residual function $r_i(\mathbf{x})$ is a nonlinear function of x and y . Therefore, the problem given in Eq. (4) is an unconstrained nonlinear optimization problem and is generally known as *nonlinear least squares*. It can be solved by using any of the Newton type optimization algorithms [5]. These are iterative algorithms and require a starting point $\mathbf{x}_0 = [x_0, y_0]^T$ which is then gradually improved in each iteration until a local minimum of the above defined objective function is found.

The system of nonlinear equations given in Eq. (3) can be linearized by subtracting one of the equations from the remaining $m - 1$ equations. If we subtract the last equation from the others, this results in the following linear system,

$$\begin{aligned} (x_1 - x_m)x + (y_1 - y_m)y &= b_1 \\ (x_2 - x_m)x + (y_2 - y_m)y &= b_2 \\ &\vdots \\ (x_{m-1} - x_m)x + (y_{m-1} - y_m)y &= b_{m-1} \end{aligned} \quad (6)$$

where,

$$b_i = \frac{1}{2} \{x_i^2 - x_m^2 + y_i^2 - y_m^2 + d_m^2 - d_i^2\} \quad (7)$$

In matrix notation, the linear system given in Eq. (7) can be expressed as,

$$\mathbf{A}\mathbf{x} = \mathbf{b} \quad (8)$$

where,

$$\mathbf{A} = \begin{bmatrix} x_1 - x_m & y_1 - y_m \\ x_2 - x_m & y_2 - y_m \\ \vdots & \vdots \\ x_{m-1} - x_m & y_{m-1} - y_m \end{bmatrix} \quad (9)$$

and

$$\mathbf{b} = \frac{1}{2} \begin{bmatrix} x_1^2 - x_m^2 + y_1^2 - y_m^2 + d_m^2 - d_1^2 \\ x_2^2 - x_m^2 + y_2^2 - y_m^2 + d_m^2 - d_2^2 \\ \vdots \\ x_{m-1}^2 - x_m^2 + y_{m-1}^2 - y_m^2 + d_m^2 - d_{m-1}^2 \end{bmatrix} \quad (10)$$

The system of linear equations given in Eq. (7) can be solved for x and y by using the least squares approach given in Eq. (4) with the following residual function,

$$r_i(\mathbf{x}) = (x_i - x_m)x + (y_i - y_m)y - b_i \quad i = 1, \dots, m - 1 \quad (11)$$

When this residual function which is linear in the unknowns x and y is used, the problem expressed in Eq. (4) is known as *linear least squares* and has a closed form solution given as,

$$\hat{\mathbf{x}} = \left(\mathbf{A}^T \mathbf{A}\right)^{-1} \mathbf{A}^T \mathbf{b} \quad (12)$$

If $\bar{\mathbf{b}}$ is a vector created by using the true distances \bar{d}_i in Eq. (10), the localization error can be given as,

$$\|\mathbf{x} - \hat{\mathbf{x}}\|_2 \leq \|\mathbf{A}^\dagger\|_2 \|\mathbf{v}\|_2 \quad (13)$$

where \mathbf{v} is the discrepancy or the error,

$$\mathbf{v} = \bar{\mathbf{b}} - \mathbf{b} \quad (14)$$

$$\mathbf{A}^\dagger = \left(\mathbf{A}^T \mathbf{A}\right)^{-1} \mathbf{A}^T \quad (15)$$

Eq. (13) suggests that even if one of the estimated ranges contains a large error, it will significantly increase the vector norm $\|\mathbf{v}\|_2$ and thus the upper bound on the localization error. Although, we have used the closed form solution

of linear least squares to explain this, the nonlinear least squares of Eq. (4) also suffers from this shortcoming. Thus the traditional approach of least squares based localization will not be able to localize sensor nodes accurately in non line of sight prone cluttered environment where some of the range measurements can be erroneous.

4. ROBUST LOCALIZATION

In this section, we present our robust localization algorithm. We have observed in the previous section that each range estimate between anchor nodes and the node with unknown coordinates can be represented as an Euclidean distance function resulting in a system of nonlinear equations given in Eq. (3). It is generally desirable to convert a nonlinear system of equations into a linear one. Nonlinear equation systems can have multiple roots and local minima. This presents a significant challenge to the optimization algorithms that have to rely on heuristics or additional application knowledge which might not be readily available to guide them towards the appropriate solution. However, when dealing with linear equation systems, we can leverage the very well developed field of linear algebra. Therefore, we would like to convert the nonlinear equation system given in Eq. (3) into a linear system. We have already illustrated one approach in the previous section that can be used to accomplish this where one of the equations is subtracted from the rest to eliminate the nonlinear terms. This results in a linear system given in Eq. (7). Another similar approach is to subtract each equation from the rest, thus providing $\binom{m}{2}$ distinct linear equations. However, such approaches of linearization are unsuitable for our particular scenario where some of the range measurements contain large non line of sight errors. If an equation representing the range measurement with large error is chosen to be subtracted from the rest, it will result in corrupting all the linear equations. However, we can avoid this by re-writing the nonlinear equations of the system given in Eq. (3) as follows,

$$\begin{aligned} -2x_1x - 2y_1y + v &= b_1 - n_1 - e_1 \\ -2x_2x - 2y_2y + v &= b_2 - n_2 - e_2 \\ &\vdots \\ -2x_mx - 2y_my + v &= b_m - n_m - e_m \end{aligned} \quad (16)$$

where

$$\begin{aligned} v &= x^2 + y^2 \\ b_i &= d_i^2 - x_i^2 - y_i^2 \\ n_i &= \bar{n}_i^2 + 2\bar{d}_i\bar{n}_i \\ e_i &= 2d_i\bar{e}_i - \bar{e}_i^2 \end{aligned} \quad (17)$$

Since $\bar{e}_i \ll d_i$, we have,

$$e_i \approx 2d_i\bar{e}_i \quad (18)$$

Therefore, each range measurement equation is kept independent of others and the nonlinearity is hidden in a new variable v . Eq. (16) can be written in matrix notation as,

$$\mathbf{A}\mathbf{x} + \mathbf{n} + \mathbf{e} = \mathbf{b} \quad (19)$$

where $\mathbf{A} \in \mathbb{R}^{m \times 3}$ is given as,

$$\mathbf{A} = \begin{bmatrix} -2x_1 & -2y_1 & 1 \\ -2x_2 & -2y_2 & 1 \\ \vdots & \vdots & \vdots \\ -2x_m & -2y_m & 1 \end{bmatrix} \quad (20)$$

$$\mathbf{b} = \begin{bmatrix} d_1^2 - x_1^2 - y_1^2 \\ d_2^2 - x_2^2 - y_2^2 \\ \vdots \\ d_m^2 - x_m^2 - y_m^2 \end{bmatrix}, \mathbf{x} = \begin{bmatrix} x \\ y \\ v \end{bmatrix}, \quad (21)$$

and \mathbf{n} and \mathbf{e} are vectors of scaled non line of sight and measurement errors respectively. Eq. (19) has two unknowns, the node coordinates \mathbf{x} and the scaled non line of sight errors \mathbf{n} whereas \mathbf{e} is a vector of Gaussian random variables. If we have an estimate $\hat{\mathbf{n}}$ of the scaled non line of sight errors, we can compute an estimate of the node coordinates as,

$$\hat{\mathbf{x}} = \left(\mathbf{A}^T \mathbf{A}\right)^{-1} \mathbf{A}^T (\mathbf{b} - \hat{\mathbf{n}}) \quad (22)$$

We assume that the anchor nodes are placed in such a manner that they are non-collinear and thus the rank of matrix \mathbf{A} is 3. If \mathbf{Z} is an orthonormal basis of the null space of \mathbf{A}^T then

$$\mathbf{Z}^T \mathbf{A} = 0 \quad (23)$$

where $\mathbf{Z} \in \mathbb{R}^{m \times m-3}$. Let us suppose that $\mathbf{C} = \mathbf{Z}^T$ and premultiply Eq. (19) with \mathbf{C} . This annihilates the matrix \mathbf{A} and the unknown coordinates \mathbf{x} and we are left with,

$$\mathbf{C}\mathbf{n} + \tilde{\mathbf{e}} = \mathbf{y} \quad (24)$$

where $\mathbf{C} \in \mathbb{R}^{m-3 \times m}$ and

$$\mathbf{y} = \mathbf{C}\mathbf{b} \quad (25)$$

$$\tilde{\mathbf{e}} = \mathbf{C}\mathbf{e} \quad (26)$$

According to the property of vector norm,

$$\|\tilde{\mathbf{e}}\|_2 \leq \|\mathbf{C}\|_2 \|\mathbf{e}\|_2 \quad (27)$$

Since the rows of \mathbf{C} are orthonormal, we have $\|\mathbf{C}\|_2 = 1$ and thus,

$$\|\tilde{\mathbf{e}}\|_2 \leq \|\mathbf{e}\|_2 \quad (28)$$

Since \mathbf{e} is a random Gaussian vector, the norm $\|\mathbf{e}\|_2 = \sqrt{\sum_i e_i^2}$ is a random variable with Chi distribution. The mean μ_e of this random variable is given as,

$$\mu_e = \sqrt{2} \frac{\Gamma((m+1)/2)}{\Gamma(m/2)} \quad (29)$$

Thus the only unknown in Eq. (24) is the vector \mathbf{n} . If we can find a unique solution $\hat{\mathbf{n}}$ which is in fact an estimate of non line of sight errors, we can compute the unknown node coordinates using Eq. (22). However, Eq. (24) is an underdetermined system of linear equations with an infinite number of solutions because the number of unknowns

is larger than the number of available equations. We can, however, find a way of determining the vector \mathbf{n} of scaled non line of sight errors if we impose certain constraints on it. If we assume that the vector \mathbf{n} is *sparse* i.e. the majority of its elements are zero, then it is possible to find a unique solution $\hat{\mathbf{n}}$ by solving the following problem.

$$\begin{aligned} & \text{minimize} && \|\mathbf{n}\|_1 \\ & \text{subject to} && \|\mathbf{C}\mathbf{n} - \mathbf{y}\|_2 \leq \|\mathbf{e}\|_2 \end{aligned} \quad (30)$$

where we have used Eq. (28) to replace $\|\tilde{\mathbf{e}}\|_2$ with $\|\mathbf{e}\|_2$ in the above problem and it can be determined using Eq. (29). This is a convex optimization problem and can be easily solved using second-order cone programming [7]. Our assumption that \mathbf{n} is sparse in fact means that we are assuming that the majority of the range measurements are direct line of sight and only a few of the estimated distances contain large non line of sight errors. In the next section, we will quantify this statement and explicitly state the percentage of the range measurements corrupted by non line of sight errors that our proposed approach can withstand. Another extremely important observation is the fact that non line of sight signal propagation always elongates the estimated distances i.e. the non line of sight errors are always positive. We can use this extra information to further constrain the optimization problem presented in Eq. (30). The new optimization problem is given as,

$$\begin{aligned} & \text{minimize} && \|\mathbf{n}\|_1 \\ & \text{subject to} && \|\mathbf{C}\mathbf{n} - \mathbf{y}\|_2 \leq \|\mathbf{e}\|_2 \\ & && \mathbf{n} \geq 0 \end{aligned} \quad (31)$$

In the following sections, we will show that these positivity constraints $\mathbf{n} \geq 0$ are extremely important in increasing the robustness of our proposed approach to erroneous non line of sight range measurements.

This approach of determining sparse solutions of underdetermined linear systems using l_1 -norm minimization is known as *Basis Pursuit* [10]. Since its recent discovery, it has found applications in a wide spectrum of areas ranging from compressive sensing, signal and image processing, statistics, medical imaging, error correction, interference rejection and many more. It has also made possible some fascinating new applications that were not possible before. For example, dynamic images of beating heart using magnetic resonance imaging. However, to the best of our knowledge, it has never been used to mitigate the effect of non line of sight errors for localization in cluttered environments. Our work shows that by leveraging these developments in other fields, we can localize sensor nodes even in extremely harsh environments where the currently available approaches are not successful.

5. ROBUSTNESS ANALYSIS

Naturally the very first question that comes to mind is how robust is the proposed approach? That is, given a set of reference nodes and distance estimates to these reference nodes, what is the largest percentage of erroneous range measurements that our proposed algorithm can tolerate before breaking down completely. In this section, we answer this question and quantify this breaking point. Let us consider a noiseless underdetermined system as,

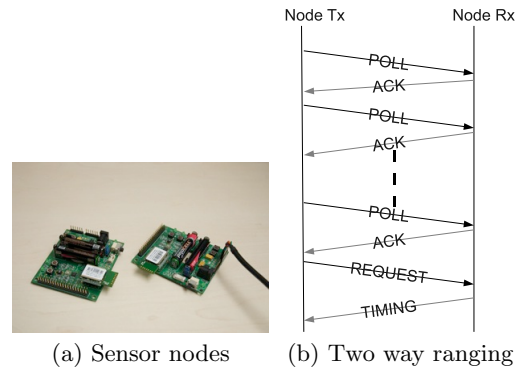


Figure 3: Jennic JN5148 radio ranging nodes

$$\mathbf{G}\mathbf{h} = \mathbf{c} \quad (32)$$

where $\mathbf{G} \in \mathbb{R}^{p \times q}$ with $p < q$ and the unknown vector \mathbf{h} is non-negative and *s-sparse* i.e., only s elements of \mathbf{h} are non-zero and positive. We can determine an estimate $\hat{\mathbf{h}}$ of vector \mathbf{h} using a convex program similar to Eq. (31) as,

$$\begin{aligned} & \text{minimize} && \|\mathbf{h}\|_1 \\ & \text{subject to} && \mathbf{G}\mathbf{h} = \mathbf{c} \\ & && \mathbf{h} \geq 0 \end{aligned} \quad (33)$$

Donoho and Tanner [14] studied this problem using convex polytope theory. They established that the vector $\hat{\mathbf{h}}$ obtained by solving the above convex program is unique if the number of faces of a convex polytope P when projected down to \mathbb{R}^p from \mathbb{R}^q remain unchanged. By using the classical results on counting the faces of randomly projected convex polytopes by Affentranger and Schneider [4] and by Vershik and Sporyshev [26], they were able to show that under asymptotic conditions this happens when

$$s \leq \frac{p}{2} + 1 \quad (34)$$

This shows that almost half of the elements of \mathbf{h} can be non-zero and the above convex program will still be able to recover it. However, when the positivity constraints $\mathbf{h} \geq 0$ are removed from Eq. (33), the threshold for the successful recovery of \mathbf{h} is lowered to

$$s \leq \frac{p+1}{3} \quad (35)$$

This suggests that the positivity constraints are extremely important for successful recovery of unique sparse solutions of underdetermined systems.

Here we must point out that the above results were derived for the noise-free version of the problem given in Eq. (33) with equality constraints. However, in practice we have to deal with noise and solve Eq. (31) that involves conic constraints. In an extended work, Donoho and Tanner [15] suggest that these results are applicable to the noisy version of the problem as well. Donoho et al. [13] have also shown this analytically when \mathbf{G} is a partial Fourier matrix.

In order to derive these results, it was also assumed that the size of the problem (the matrices and vectors in Eq. (33))

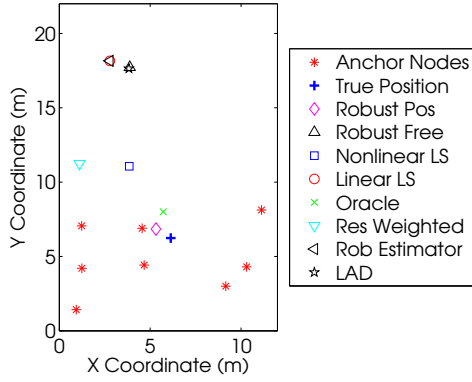


Figure 4: Localizing a sensor node in a room using Jennic radio ranging

tends to infinity. Donoho and Tanner [12] have derived some non-asymptotic results as well but these results still require the dimensions of \mathbf{G} to be on the order of several hundreds which is not possible for our particular application. Turning back to our localization approach described in the previous section, we can use asymptotic results to describe the upper bounds of its robustness. Thus for the convex program in Eq. (31), we have

$$s \leq \frac{m-1}{2} \quad (36)$$

and for Eq. (30),

$$s \leq \frac{m-2}{3} \quad (37)$$

These results suggest that our convex programming based robust localization approach will be able to estimate the non line of sight errors accurately even if almost half of the measurements are erroneous. If, however, the positivity constraints on the errors are removed, robustness is significantly reduced and only one third of the erroneous measurements can be corrected. In the later sections, we will show through experimental results that even for a small number of anchor nodes, our localization algorithm is robust in the presence of as many as 40% erroneous measurements.

6. EXPERIMENTS

In this section, we present results from the experiments that were conducted to assess the performance of our convex programming based robust localization algorithm. We compare the localization error of our approach which we refer to as *Robust Pos* with seven different algorithms. These include 1) *Nonlinear LS*: the nonlinear least squares approach of Eq. (4), 2) *Linear LS*: linear least squares with the linearization discussed in Section 4, 3) *Robust Free*: convex program of Eq. (30) that does not include the positivity constraints on non line of sight errors in the problem formulation, 4) *Oracle*: an oracle that has the complete knowledge about which range measurements are due to non line of sight signals. It removes such erroneous measurements and then calculates the node position using linear least squares. 5) *Res Weighted* the residual weighted algorithm by Chen [9] for localization in NLOS environments, 6) *Rob Estimator*

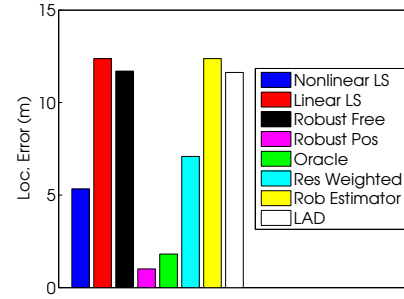


Figure 5: Localization error for various algorithms

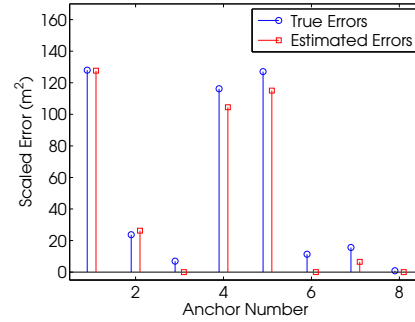


Figure 6: Comparison of true errors and the errors estimated by our algorithm

the robust estimator for localization proposed by Casas et al. [8] and 7) *LAD* the least absolute deviation based approach from statistics for solving linear equation systems with large errors. In the following subsections, we describe our experiments from three different hardware platforms.

6.1 Radio Ranging

In this section, we present our results from experiments that were carried out with sensor nodes that use 2.4GHz radio ranging to estimate distance between themselves. For these experiments we used JN5148 sensor nodes shown in Fig. (3a) from Jennic [1]. These nodes estimate the distance by measuring time of flight of radio packets between two nodes. A transmitter node sends out a POLL packet and the receiving node responds with an ACK. It also measures the turnaround time in hardware for it to respond to the POLL message as shown in Fig. (3b). At the transmitter the total time along with this turnaround time gives an estimate of two way time of flight between the nodes. When issued with a ranging command, the transmitter node performs a burst of 10 measurements. The receiver records the turnaround times of all 10 packets. This information is then sent back to the transmitter in a separate data packet. The transmitter then estimates the distance using the timing information. This is known as forward ranging. Since the estimated times can be affected by the clock offsets and accuracies, a reverse burst can also be performed where the transmitter and the receiver nodes swap roles.

Our experience with these sensor nodes suggests that they perform very well in an open outdoors environment where they can measure distances of up to 100m with an accuracy

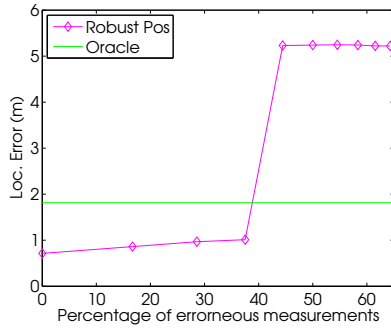


Figure 7: Empirical evidence of the breakdown threshold

of less than 1m. However, when these nodes are used in an ordinary indoors environment, some of the range measurements can have errors of up to 100%. This is due to the fact that in an indoors environment, the radio signal can reflect and bounce off the walls or the furniture and the physical layer at the receiver can lock onto any of the reflected signals. This creates a very harsh scenario where some of the range measurements are very accurate with less than 1m error whereas others can have errors of several tens of meters and no other information is available to distinguish between the erroneous and good range measurements.

This experiment was performed in a 15m \times 10m lecture theater full of chairs and other furniture. One sensor node was connected to the laptop to record the range measurements and a second node which was used as a reference node was placed at different positions inside the lecture theater. At each position, its coordinates were measured using a laser range finder and 100 forward and 100 reverse range measurements were performed to the sensor node connected to the laptop. A mean of these measurements was used as an estimate of the measured range between the two sensor nodes. The recorded reference node coordinates and the range measurements were then used to localize the sensor node connected to the laptop using different localization algorithms. Fig. (4) shows one scenario with 8 reference node positions shown with red stars and the true position of the sensor node connected to the laptop is shown as a blue cross. In this set up 5 of the range measurements were accurate whereas the remaining 3 had significant errors. In the figure, the estimate of the position computed by our robust localization approach is shown as a magenta diamond. The coordinates determined by the algorithm without the positivity constraints, nonlinear least squares, linear least squares and the oracle algorithm are shown as a black triangle, a blue square, a red circle and a green cross respectively. The position estimate computed using the residual weighted approach of Chen [9], the robust estimator of Casas et al. [8] and the least absolute deviation estimator are shown as cyan inverted triangle, a black left triangle and a black pentagram respectively.

The localization error for our approach is about 1m and that of the oracle is 1.8m! The reason for this is that our algorithm corrects the erroneous measurements and then uses all the reference node positions and the corrected measurements to estimate the node coordinates whereas the oracle removes the bad measurements and uses the remaining ones



Figure 8: MIT Cricket notes

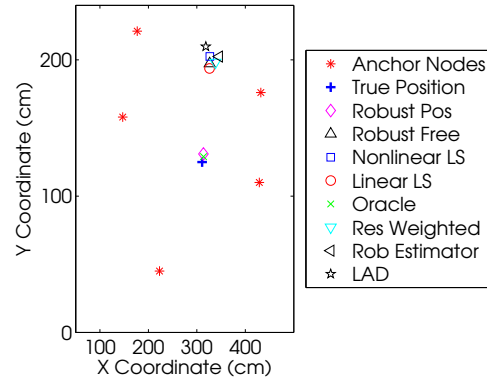


Figure 9: Localizing a sensor node in a room using ultrasound ranging

to calculate the node coordinates. Fig. (5) compares the localization errors of our approach with all of the other approaches. Since the residual weighted algorithm computes the position estimate as a weighted linear combination of the solutions of all the subsets of range measurements, those corrupted by NLOS errors influence the final position estimate and thus cause the higher localization error. The robust estimator approach also examines the subsets of measurements and tries to filter out the erroneous measurements by comparing the residuals with a threshold. In this experiment, all the residuals were below the computed threshold and thus the algorithm failed to detect erroneous measurements. This resulted in the large localization error. The least absolute deviation estimator also could not perform significantly better.

Fig. (6) compares the actual errors for every reference node with an estimate \hat{n} of the errors computed by our algorithm. This shows that the estimated errors are quite similar to the actual errors and this is the reason for the good performance of our algorithm because these estimated errors are removed before calculating the node coordinates as shown in Eq. (22). We must point out that these are scaled non line of sight errors n_i as opposed to non line of sight errors \tilde{n}_i . Eq. (18) shows how non line of sight errors are scaled by true distance to form these scaled errors.

In order to empirically test the breaking point of our algorithm, we conducted another experiment in the same lecture theater. In this experiment, we kept the 5 good range measurements and the reference positions and gradually in-

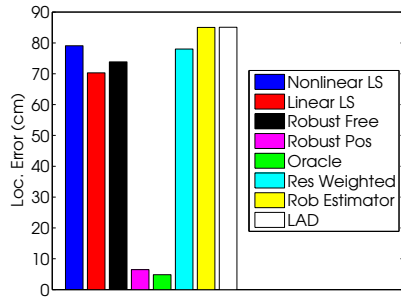


Figure 10: Localization errors of various algorithms

creased the number of erroneous measurements from 0 to 9 by placing the reference node at different locations in the room. Thus the total number of reference positions and the measurements varied from 5 to 14 with the percentage of the erroneous measurements varying from 0% to 65%. Fig. (7) shows the localization error versus the percentage of erroneous measurements. It clearly shows a *knee* where just after 40%, the error jumps from less than 1m to more than 5m. This is due to the fact that the sparsity constraint on \mathbf{n} is violated and convex programming is unable to find a unique solution to the underdetermined system of Eq. (24). The performance of the oracle algorithm is also shown for comparison and we can see that our algorithm performs better than the oracle before the breakdown point is reached. This suggests that our algorithm will perform better than any of the approaches that try to distinguish between the line of sight and non line of sight measurements unless additional knowledge about the non line of sight errors is incorporated in them. Our approach implicitly does this by automatically *inferring* this knowledge instead of relying on the user to provide it. However, it is only successful in inferring this knowledge if the number of non line of sight measurements is less than half.

6.2 In Air Acoustic Ranging

In this section, we outline the results of our experiments that were carried out using MIT Cricket notes [22]. These notes use time difference of arrival between a radio signal and an ultrasound signal to estimate the distance. A transmitter sends out a radio packet and ultrasound pulse simultaneously. Since the speed of propagation of radio waves is significantly higher than the speed of sound, it is received almost instantaneously by the receiver. It starts a timer and on receiving the ultrasound pulse, this timer is stopped. This gives an estimate of one way time of flight which is then used with the speed of propagation of sound to determine the distance to the transmitter. In these experiments 7 notes were placed in an office in a 3m \times 3m area as shown in Fig. (8). One of the notes was programmed to act like a receiver and the other 6 worked like beacons or reference nodes continuously sending out radio and ultrasound signals. The receiver used this transmitted signals to estimate distances to each of the reference nodes. The receiver was also connected to a laptop computer to record all the measurements.

Since the ultrasound pulses emitted by the notes can reflect and bounce off solid place surfaces, we placed two notes in such a manner that they were facing a wall. This created

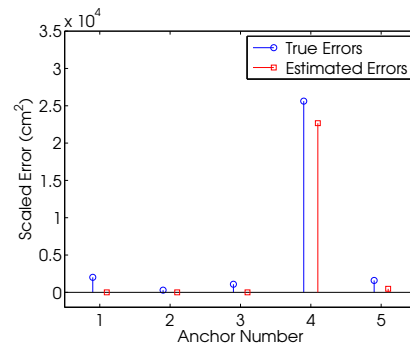


Figure 11: Comparison of true and estimated errors

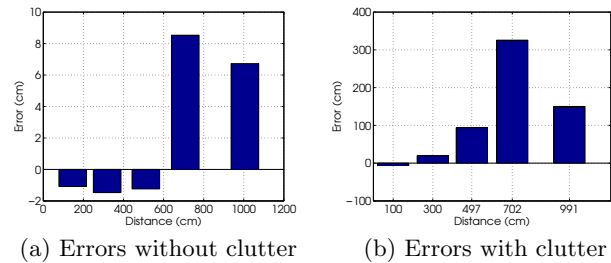


Figure 12: Ranging errors for clear and cluttered underwater environment

non line of sight propagation of ultrasound pulses emitted by these notes and thus the distances to these reference nodes were overestimated by the receiver. For each of these transmitters, the overestimation error is around 70cm. For the first experiment, one of these non line of sight nodes was switched off. Therefore, there were a total of 5 transmitters or reference nodes and only one of these was generating non line of sight signals. At the receiver, distances to all 5 transmitters were estimated and then along with the transmitter nodes coordinates used to determine the location of the receiver using the above mentioned localization approaches.

Fig. (9) shows the scenario with 5 reference node positions, the true position of the receiver and the coordinates calculated by our algorithm and other approaches. It shows that the receiver position determined by our algorithm and the oracle is almost indistinguishable from the true position. The localization error for our approach is 6.3cm and that of the oracle is 4.9cm. Thus despite having an erroneous measurement with an error of almost 70cm, our algorithm comes as close as about a 1cm of the oracle. The robust estimator removes two of the good measurements and accepts one erroneous range measurement for its final coordinate computation and thus exhibits a large error. The residual weighted algorithm and least absolute deviation also results in large localization errors. Fig. (10) compares the localization errors of all of the tested algorithms.

The reason that our algorithm was able to perform as well as the oracle is that it was able to estimate the errors very accurately. Fig. (11) compares the actual errors scaled by the true distance and the estimate of these errors computed by our algorithm. It shows that the estimate matches the true values quite reasonably. Since these errors are removed before computing the node coordinates, the calculated node

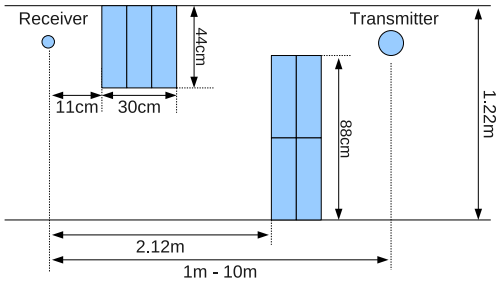


Figure 13: Top down view of the tank containing clutter

position is quite close to the actual position of the receiver.

In the second experiment, the second transmitter with non line of sight signals was also switched on. Thus there were a total of 6 reference nodes in this experiment with 2 being non line of sight. Thus 33.3% of the measurements were erroneous. In this experiment, the localization error of our algorithm jumped to 120cm which indicates that it had moved beyond the breakdown point and was thus unable to determine a unique estimate \hat{n} of errors. We notice that the breakdown point in this experiment was at 33.3% which is lower than the 40% that was observed in the previous experiment. This is due to the fact that the number of anchor nodes and thus the size of the underdetermined system of Eq. (24) was smaller for this experiment as compared to the previous one. The results presented in Section 5 suggest that as we increase the number of anchor nodes, the breakdown point of the algorithm approaches 50%.

6.3 Underwater Acoustic Ranging

We now present some underwater experiments where ultrasound signals from underwater acoustic transducers were used to perform range measurements. Since our robots are still in a prototype stage, we used two acoustic transducers connected to a desktop computer with the help of a ADC/DAC card and the signal waveforms were generated from LabView software. We chose to use Neptune T204 [2] as a transmitter due to its hemispherical beam pattern and 40KR08 [3] was used as a receiver. We are considering to use T204 for reference nodes fixed to the pond infrastructure and 40KR08 for our mobile sensor nodes because of its small size. These transducers were connected to two separate metal frames which could be moved on top of a lab tank with the transducers positioned inside the water. The dimensions of the tank are 12m×1.2m×0.6m.

For these experiments, an MLS coded BPSK signal with a code length of 2047bits was used for ranging because such signals are better suited to combat multipath and interference rejection. A carrier frequency of 50kHz was selected after inspecting the frequency response of both the transducers. The signal to be transmitted was generated by the desktop computer, converted to analogue using a 12bit digital to analogue converter on the card and then fed into the transducer. At the receiver, the received signal was amplified through a 48.4dB gain amplifier, digitized through a 16bit ADC and then cross correlated in software at the desktop computer with transmitted signal to detect the first arriving peak to the signal. This provided us with the time of the flight of the signal from the transmitter to the receiver. During the experiments, the water temperature was

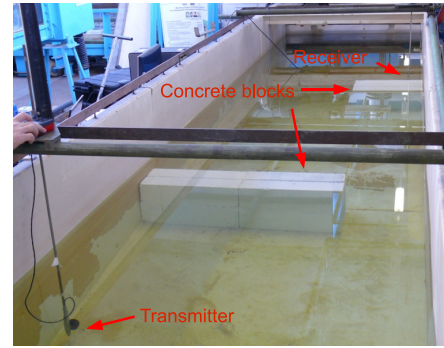


Figure 14: Experimental set up for non line of sight conditions

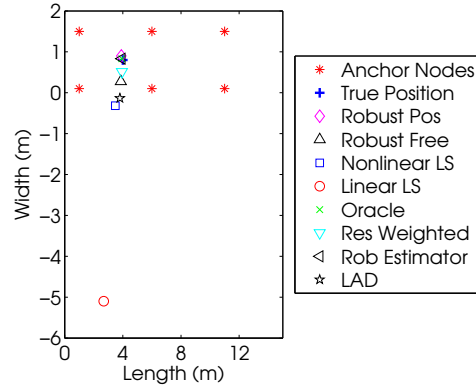


Figure 15: Simulated localization in water tank

measured with a thermometer and was found to be constant 18°C. According to Lubbers and Graaff [20] equation,

$$V_{us} = 1405.03 + 4.624t - 0.0383t^2 \quad (38)$$

the speed of propagation of ultrasound in water at this temperature is 1475.85m/s. Eq. (38) is valid for a temperature range of 10 – 40°C at atmospheric pressure. Using this speed of propagation, the measured time of flight was then converted into a range estimate.

For the first experiment, both the receiver and the transmitter was placed close to the walls of the tank with clear line of sight. The distance between the transmitter and the vessel wall was 6cm and similarly the receiver was 9cm away from the wall. The depth of both transducers was 1.5m. The transducers were placed close to the walls to observe if such boundary conditions could give rise to strong multipath propagation of acoustic signals. The receiver was fixed, whereas the transmitter was positioned at different distances from the receiver along the length of the tank. At each transmitter location, MLS coded BPSK signals were transmitted and 100 range estimates were recorded. Fig. (12a) shows the ranging errors for this obstacle free scenario. It shows that under line of sight conditions, the range measurements have very small errors on the order of few centimeters even when the distance between the two transducers is 10m.

In order to observe the effect of solid occlusions on the ranging system, two sets of concrete blocks were placed inside the tank between the transmitter and the receiver as

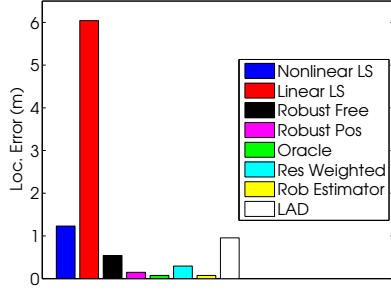


Figure 16: Localization errors of various algorithms

shown in Fig. (13). And again the transmitter was positioned at different locations along the length of the tank and 100 range estimates were recorded for each transmitter position. Fig. (14) shows the actual experimental set up. In this case, we observed large errors in the estimated distances ranging from less than 1m to 3m. When the separation between the receiver and the transmitter is 1m, we observe that the signal is strong enough to pass through the porous concrete and thus results in a small error of few centimeters. We can use the error distributions for the obstruction free and obstructed case from Fig. (12a) and Fig. (14) respectively to emulate the performance of this underwater ranging system for localizing a mobile sensor node. Let us take a simplified view of the underwater sensor network and suppose that there are five reference nodes equipped with T204 transducers fixed with in this tank and a robot equipped with 40KR08 estimates distances to these six anchor nodes as shown in Fig. (15). Let us suppose that one of these anchor nodes results in a non line of sight range estimate with an error randomly chosen from a uniform distribution $\mathcal{U}(a, b)$ with $a = 0.5\text{m}$ and $b = 3\text{m}$ and line of sight measurement errors are from $\mathcal{N}(0, \sigma^2)$ with $\sigma = 4\text{cm}$. Fig. (15) shows the estimated positions and Fig. (16) presents the localization errors of all of the considered algorithms. These results show that when this underwater ranging system will be employed for localization in this particular environment, our algorithm will be able to successfully localize the sensor nodes. Although, this is not our target application environment, such error distributions from any of the storage pools can be used to verify the performance of our algorithm and we consider these experiments as a preliminary step towards that goal.

7. MOBILE SENSOR NODES

In this section, we focus on the localization of mobile sensor nodes and compare the performance of our algorithm with an Extended Kalman Filter. A Kalman filter is considered state of the art in estimating the state of a dynamic system. It uses a state model to predict the state of the system, which is then combined with the measurements in a least squares sense according to the covariances of both the predicted state and the measurements. We assume that a sensor node is moving with a constant velocity in the cluttered environment. At each discrete time step k , it estimates its distance from the fixed anchor nodes deployed in the environment. The system state that we want to estimate using a Kalman filter is the coordinates of the sensor node as it

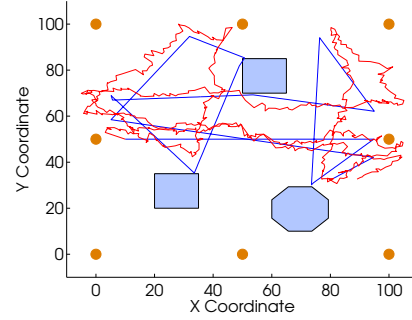


Figure 17: Kalman filter

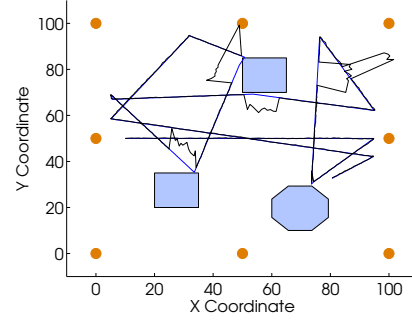


Figure 18: Robust localization

moves around in the pond. Let us suppose that \mathbf{x}_k is a vector of the current state at time step k . Eq. (39) is a state equation that relates the current state to the previous one,

$$\mathbf{x}_k = \mathbf{F}\mathbf{x}_{k-1} + \mathbf{G}\mathbf{u} + \mathbf{w} \quad (39)$$

$$\mathbf{F} = \begin{bmatrix} 1 & 0 \\ 0 & 1 \end{bmatrix}, \mathbf{G} = \begin{bmatrix} k & 0 \\ 0 & k \end{bmatrix}, \mathbf{u} = \begin{bmatrix} u_x \\ u_y \end{bmatrix} \quad (40)$$

where u_x and u_y are the x and y components of the velocity and \mathbf{w} is a gaussian random vector with covariance \mathbf{W} . It represents the noise in our chosen state model i.e. a sensor node moving with constant velocity. At each time step k , the sensor node also estimates its distances to the fixed reference nodes which results in a nonlinear equation system given in Eq. (3). We can represent this as,

$$\mathbf{d}_k = h(\mathbf{x}_k, \epsilon_k) \quad (41)$$

where \mathbf{d}_k is a vector of range measurements and h is a nonlinear function that relates the current state and measurement noise ϵ_k with covariance \mathbf{E} to the measurements. We use the following standard Kalman filter equations to estimate the node coordinates at each time step k .

$$\begin{aligned} \mathbf{x}_{k|k-1} &= \mathbf{F}\mathbf{x}_{k-1|k-1} + \mathbf{G}\mathbf{u} \\ \mathbf{P}_{k|k-1} &= \mathbf{F}\mathbf{P}_{k-1|k-1}\mathbf{F}^T + \mathbf{W} \\ \mathbf{K}_k &= \mathbf{P}_{k|k-1}\mathbf{H}_k^T(\mathbf{H}_k\mathbf{P}_{k|k-1}\mathbf{H}_k^T + \mathbf{E})^{-1} \\ \mathbf{x}_{k|k} &= \mathbf{x}_{k|k-1} + \mathbf{K}_k(\mathbf{d}_k - h(\mathbf{x}_{k|k-1}, 0)) \\ \mathbf{P}_{k|k} &= (\mathbf{I} - \mathbf{K}_k\mathbf{H}_k)\mathbf{P}_{k|k-1} \end{aligned} \quad (42)$$

where \mathbf{H}_k is the jacobian of h at the current estimated state. The $k|k-1$ is the standard notation of the filter theory and can be thought of as an estimate of the subscripted quantity at time step k using the information from $k-1$. The matrix \mathbf{K} is known as Kalman gain and \mathbf{P} is the covariance of the state estimate.

As compared to the Kalman filter, our approach does not require the state model or any information about the robot movement. At each time step k , it only uses the available range measurements and the reference node coordinates to estimate the robot position using Eq. (31).

Fig. (17) shows a simulated scenario where a sensor node has been moving in a cluttered environment. The orange circles indicate the positions of reference nodes and the clutter is shown as blue polygons. As the node moves around, it estimates its position using the Extended Kalman filter described above. For these simulations, the covariances of the model noise and measurement noise were $\mathbf{W} = \begin{bmatrix} 0.01 & 0 \\ 0 & 0.01 \end{bmatrix}$

and $\mathbf{E} = \begin{bmatrix} 0.01 & 0 \\ 0 & 0.01 \end{bmatrix}$ respectively and non line of sight errors were randomly selected from a uniform distribution with $a = 10$ and $b = 20$ units. The true path of the mobile node is shown in blue and the path estimated by the Kalman filter is shown in red. Although this path somewhat follows the true path of the mobile node, we can see that it contains significant errors. This is due to the fact that despite employing the dynamic state model, the Kalman filter is unable to cope with the erroneous range measurements. This sort of behaviour is expected because a Kalman filter is an extension of the least squares principle to the dynamic case.

Fig. (18) shows the same scenario when our robust localization approach is used to estimate the mobile node coordinates. As before, the true path is shown in blue and the path estimated by our approach is shown in black. As we can see from the figure, these two are almost indistinguishable for the most of the path length. However, if the robot moves to a position in the environment where the majority of the range measurements become non line of sight, our approach also breaks down because the sparsity conditions are violated and it is unable to find a unique estimate of non line of sight errors. Fig. (19) shows the localization error of both of the approaches over the entire duration of the experiment. It shows that the discrepancy between the true position of the sensor node and the location estimated by our approach is negligible most of the time.

8. RELATED WORK

Sensor network localization has received considerable attention and there is a large body of research available addressing this problem. However, we will restrict ourselves to localization under NLOS conditions. Localization in the presence of NLOS measurements has mostly been studied for cellular networks [28, 27]. A vast majority of this work assumes that it is possible to identify NLOS measurements by inspecting the statistics of a series of measurements from a mobile node [6, 19]. Once identified, these measurements can be completely removed, assigned lower weights or if NLOS error statistics are available, these can be combined with the measurements to estimate the position [11]. However, if the nodes are stationary or moving very slowly then it is not possible to use such approaches. An approach

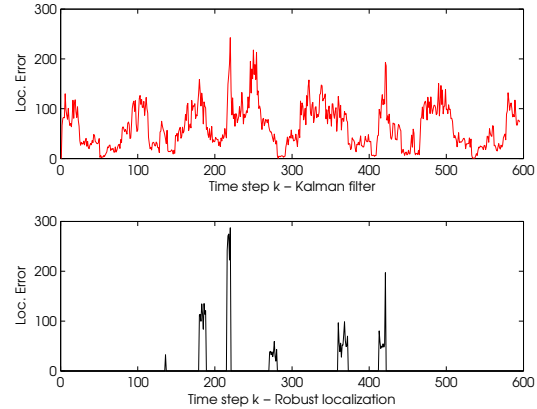


Figure 19: Comparison of localization error

that only relies on the measurements to identify and remove NLOS ranges has also been proposed [9]. However, it is computationally very expensive and it relies on heuristics that fail when there are more than one NLOS measurements present. Another similar approach [8] tries to remove the erroneous measurements by inspecting residuals. However, such an approach can also fail when the number of measurements is small.

With recent developments in UWB radio technology, NLOS localization for sensor nodes in indoor cluttered environments has also been explored [16]. However, such approaches also rely on the characteristics of the UWB signals to identify LOS and NLOS signals [24]. Just like cellular networks, after the identification, such measurements can be either removed completely or incorporated in localization [17, 25]. Another approach that has been explored is to characterize the indoor environment and then use the collected NLOS error statistics as prior information during localization [18]. However, this requires extensive pre-deployment measurements and thus cannot be used for ad-hoc networks. An approach that is similar to our work has also been proposed [21]. It treats the erroneous measurements as outliers but does not impose positivity constraints on these outliers. As we have shown, the positivity constraints on NLOS measurements are extremely important and significantly improve the performance.

9. CONCLUSION

In this paper, we presented a robust localization algorithm for determining the coordinates of sensor nodes in a cluttered environment where due to non line of sight signal propagation some of the range measurements are erroneous. We also analyzed the robustness of this algorithm both theoretically and empirically and showed that under realistic conditions, it can accurately localize sensor nodes even if as many as 40% of the range measurements are erroneous. Below this threshold, our algorithm even outperforms an oracle that possess the complete knowledge of which measurements are erroneous. We showed that our approach is completely independent of the hardware used for performing range measurements and does not require any extra information that must be gathered beforehand. This makes it suitable for localizing ad-hoc sensor networks in a wide variety of environments.

10. ACKNOWLEDGEMENTS

This work is supported by the EPSRC grants EP/F064209/1 on Actuated Acoustic Sensor Networks for Industrial Processes (AASN4IP). We would also like to thank Zhigang Qu and Christos Masouros from the University of Manchester for helping us perform the underwater experiments.

11. REFERENCES

- [1] Jennic jn5148 sensor nodes.
http://www.jennic.com/products/development_kits/jn5148_evaluation_kit.
- [2] Neptune t204 acoustic transducer.
<http://www.neptune-sonar.co.uk/t204.asp>.
- [3] Sensecomp piezoelectric transducer.
<http://www.senscomp.com/kseries.htm>.
- [4] F. Affentranger and R. Schneider. Random projections of regular simplices. *Discrete and Computational Geometry*, 7:219–226, 1992. 10.1007/BF02187839.
- [5] A. Beck, M. Teboulle, and Z. Chikishev. Iterative minimization schemes for solving the single source localization problem. *SIAM J. on Optimization*, 19:1397–1416, November 2008.
- [6] J. Borras, P. Hatrack, and N. Mandayam. Decision theoretic framework for nlos identification. In *Vehicular Technology Conference, 1998. VTC 98. 48th IEEE*, volume 2, pages 1583–1587 vol.2, May 1998.
- [7] S. Boyd and L. Vandenberghe. *Convex Optimization*. Cambridge University Press, New York, NY, USA, 2004.
- [8] R. Casas, A. Marco, J. J. Guerrero, and J. Falcó. Robust estimator for non-line-of-sight error mitigation in indoor localization. *EURASIP J. Appl. Signal Process.*, 2006:156–156, January 2006.
- [9] P.-C. Chen. A non-line-of-sight error mitigation algorithm in location estimation. In *Wireless Communications and Networking Conference, 1999. WCNC. 1999 IEEE*, pages 316–320 vol.1, 1999.
- [10] S. S. Chen, D. L. Donoho, and M. A. Saunders. Atomic decomposition by basis pursuit. *SIAM J. Sci. Comput.*, 20(1):33–61, 1998.
- [11] L. Cong and W. Zhuang. Nonline-of-sight error mitigation in mobile location. In *INFOCOM 2004. Twenty-third Annual Joint Conference of the IEEE Computer and Communications Societies*, volume 1, page 659, 2004.
- [12] D. Donoho and J. Tanner. Precise undersampling theorems. *Proceedings of the IEEE*, 98(6):913–924, jun. 2010.
- [13] D. L. Donoho, I. M. Johnstone, J. C. Hoch, and A. S. Stern. Maximum entropy and the nearly black object. *Journal of the Royal Statistical Society. Series B (Methodological)*, 54(1):pp. 41–81, 1992.
- [14] D. L. Donoho and J. Tanner. Sparse nonnegative solution of underdetermined linear equations by linear programming. *Proceedings of the National Academy of Sciences*, 102(27):9446–9451, 2005.
- [15] D. L. Donoho and J. Tanner. Sparse nonnegative solution of underdetermined linear equations by linear programming. Technical report, University of Stanford, 2005.
- [16] S. Gezici, Z. Tian, G. Giannakis, H. Kobayashi, A. Molisch, H. Poor, and Z. Sahinoglu. Localization via ultra-wideband radios: a look at positioning aspects for future sensor networks. *Signal Processing Magazine, IEEE*, 22(4):70–84, July 2005.
- [17] I. Guven, C.-C. Chong, F. Watanabe, and H. Inamura. Nlos identification and weighted least-squares localization for uwb systems using multipath channel statistics. *EURASIP J. Adv. Signal Process*, 2008:36, 2008.
- [18] D. Jourdan, D. Dardari, and M. Win. Position error bound for uwb localization in dense cluttered environments. *Aerospace and Electronic Systems, IEEE Transactions on*, 44(2):613–628, April 2008.
- [19] X. Lin, L. Ju, and S. Chen. Nlos error identification and range approximation technique in cellular networks. In *Wireless Communications, Networking and Mobile Computing, 2008. WiCOM '08. 4th International Conference on*, pages 1–4, 2008.
- [20] J. Lubbers and R. Graaff. A simple and accurate formula for the sound velocity in water. *Ultrasound in medicine and biology*, 1998.
- [21] J. Picard and A. Weiss. Accurate geolocation in the presence of outliers using linear programming. In *17th European Signal Processing Conference*.
- [22] N. B. Priyantha, A. Chakraborty, and H. Balakrishnan. The cricket location-support system. In *MobiCom '00: Proceedings of the 6th annual international conference on Mobile computing and networking*, pages 32–43, New York, NY, USA, 2000. ACM.
- [23] Y. Qi and H. Kobayashi. On geolocation accuracy with prior information in non-line-of-sight environment. In *Vehicular Technology Conference, 2002. Proceedings. VTC 2002-Fall. 2002 IEEE 56th*, volume 1, pages 285–288 vol.1, 2002.
- [24] S. Venkatesh and R. Buehrer. Non-line-of-sight identification in ultra-wideband systems based on received signal statistics. *Microwaves, Antennas & Propagation, IET*, 1(6):1120–1130, Dec. 2007.
- [25] S. Venkatesh and R. M. Buehrer. A linear programming approach to nlos error mitigation in sensor networks. In *IPSN '06: Proceedings of the 5th international conference on Information processing in sensor networks*, pages 301–308, New York, NY, USA, 2006. ACM.
- [26] A. M. Vershik and P. V. Sporyshev. Asymptotic behaviour of the number of faces of random polyhedra and the neighborliness problem. *Selecta Math. Soviet*, 11:181–201, 1992.
- [27] S.-S. Woo, H.-R. You, and J.-S. Koh. The nlos mitigation technique for position location using is-95 cdma networks. In *Vehicular Technology Conference, 2000. IEEE VTS-Fall VTC 2000. 52nd*, 2000.
- [28] M. Wylie and J. Holtzman. The non-line of sight problem in mobile location estimation. In *Universal Personal Communications, 1996. Record., 1996 5th IEEE International Conference on*, volume 2, pages 827–831 vol.2, Sep-2 Oct 1996.